Journal of Alzheimer's Disease 30 (2012) 791–803
DOI 10.3233/JAD-2012-112183
IOS Press

Changes in Brain Transcripts Related to Alzheimer's Disease in a Model of HFE Hemochromatosis are not Consistent with Increased Alzheimer's Disease Risk

Daniel M. Johnstone[a,b,c,e], Ross M. Graham[f,g,h], Debbie Trinder[f,g], Carlos Riveros[b,c,d], John K. Olynyk[f,g,i,j], Rodney J. Scott[a,b,c], Pablo Moscato[b,c,d] and Elizabeth A. Milward[a,b,c,*]
[a]*School of Biomedical Sciences and Pharmacy, The University of Newcastle, Callaghan, NSW, Australia*
[b]*Hunter Medical Research Institute, New Lambton Heights, NSW, Australia*
[c]*Priority Research Centre for Bioinformatics, Biomarker Discovery and Information-Based Medicine, The University of Newcastle, Callaghan, NSW, Australia*
[d]*School of Electrical Engineering and Computer Science, The University of Newcastle, Callaghan, NSW, Australia*
[e]*Bosch Institute and Discipline of Physiology, University of Sydney, NSW, Australia*
[f]*School of Medicine and Pharmacology, University of Western Australia, Fremantle, WA, Australia*
[g]*Western Australian Institute for Medical Research, Perth, WA, Australia*
[h]*School of Biomedical Sciences, Curtin University of Technology, Bentley, WA, Australia*
[i]*Curtin Health Innovation Research Institute, Curtin University of Technology, Bentley, WA, Australia*
[j]*Department of Gastroenterology, Fremantle Hospital, Fremantle, WA, Australia*

Accepted 5 March 2012

Abstract. Iron abnormalities are observed in the brains of Alzheimer's disease (AD) patients, but it is unclear whether common disorders of systemic iron overload such as hemochromatosis alter risks of AD. We used microarrays and real-time reverse transcription-PCR to investigate changes in the brain transcriptome of adult *Hfe*$^{-/-}$ mice, a model of hemochromatosis, relative to age- and gender-matched wildtype controls. Classification by functional pathway analysis revealed transcript changes for various genes important in AD. There were decreases of up to 9-fold in transcripts for amyloid-β protein precursor, tau, apolipoprotein E, presenilin 1, and various other γ-secretase components, as well as Notch signaling pathway molecules. This included decreased transcripts for 'hairy and enhancer of split' *Hes1* and *Hes5*, downstream targets of Notch canonical signaling. The reductions in *Hes1* and *Hes5* transcripts provide evidence that the changes in levels of transcripts for γ-secretase components and Notch signaling genes have functional consequences. The effects appeared relatively specific for AD in that few genes pertaining to other important neurodegenerative diseases, notably Parkinson's disease and Huntington's disease, or to inflammation,

*Correspondence to: Dr. Liz Milward, School of Biomedical Sciences and Pharmacy MSB, University of Newcastle, Callaghan, NSW 2308, Australia. Tel.: +61 2 4921 5167; Fax: +61 2 4921 7903; E-mail: Liz.Milward@newcastle.edu.au.

ISSN 1387-2877/12/$27.50

oxidative stress, or apoptosis, showed altered transcript levels. The observed effects on AD-related gene transcripts do not appear to be consistent with increased AD risk in *HFE* hemochromatosis and might, if anything, be predicted to protect against AD to some extent. As $Hfe^{-/-}$ mice did not have higher brain iron levels than wildtype controls, these studies highlight the need for further research in models of more severe hemochromatosis with brain iron loading.

Keywords: Amyloid-β protein precursor, γ-secretase, hemochromatosis, HFE, iron, notch signaling

Supplementary data available online: http://www.j-alz.com/issues/30/vol30-4.html#supplementarydata02

INTRODUCTION

Iron is vital for brain health, being essential for oxygen transport, mitochondrial energy production, and many brain-specific functions including production of neurotransmitters and myelin. Yet excess iron can cause dysfunction or death of neurons and other brain cells [1–3].

Severe brain iron dyshomeostasis can be accompanied by serious neurologic illnesses, such as dementia or movement disorders [3, 4]. This is exemplified by the group of diseases referred to as neurodegeneration with brain iron accumulation, which includes pantothenate kinase-associated neurodegeneration and neuroferritinopathy [5, 6]. Iron abnormalities have also been detected in brains of Alzheimer's disease (AD) patients using various different techniques, including histochemical staining for iron [7, 8], magnetic resonance imaging [9, 10], and spectroscopic, tomographic, and related techniques [11]. Whether brain iron abnormalities are a primary cause of the neurologic symptoms in these and other disorders, or whether brain iron abnormalities are instead secondary epiphenomena, is still under debate.

A related area of contention is whether neurologic deficits occur in hemochromatosis, a common disorder of systemic iron overload. Hemochromatosis is characterized by increased iron absorption and iron loading in the liver and other tissues, leading to organ damage [12]. Most patients with hemochromatosis are homozygous for the C282Y polymorphism of the *HFE* gene [13]. This gene has roles in regulating dietary iron absorption in the duodenum as well as iron uptake in various other tissues [14, 15]. Around 0.5% of people of Anglo-Celtic descent are homozygous for the *HFE* C282Y polymorphism [16, 17]. Not everyone with this genotype develops an iron overload phenotype (incomplete penetrance), but 25% or more do eventually develop hemochromatosis by 'gold standard' biopsy evidence of liver fibrosis or cirrhosis [16–19].

There is little information on the prevalence and extent of abnormal brain iron deposition in people with hemochromatosis or *HFE* polymorphisms. Magnetic resonance imaging suggests some hemochromatosis patients may have abnormal iron accumulation in brain regions such as the basal ganglia [20, 21], and some asymptomatic individuals with *HFE* polymorphisms may also have region-specific increases in brain iron [22]. However, various dietary or genetic animal models of iron overload and hemochromatosis show no measurable change in brain iron levels, despite having high systemic iron levels for periods of up to at least three months [23–28].

The effects of hemochromatosis and *HFE* polymorphisms on brain function and disease risks are also not well understood. *HFE* polymorphisms have been proposed as a risk factor for AD as the chromosomal region 6p21 containing the *HFE* gene has shown genetic association to AD [29–31], and several studies investigating epistatic synergy between polymorphisms in *HFE* and the transferrin gene have provided evidence for increased risks of AD in individuals with polymorphisms in both genes [32–34]. However, while many studies have now directly investigated the association between AD and *HFE* polymorphisms alone [35–43], these have provided inconsistent results. A large, well-powered meta-analysis of eight studies comprising in total 758 AD cases and 626 controls failed to find a significant association between AD and any hemochromatosis *HFE* genotype [44]. However, the studies used for this meta-analysis did not assess penetrance, i.e., which participants with *HFE* polymorphisms had increased body iron status and therefore increased risk of iron-related disease.

One well established model of genetic iron overload and hemochromatosis is the *Hfe* knockout mouse model ($Hfe^{-/-}$), which shows systemic iron loading [45] and provides a model for investigating the effects of penetrant *HFE* polymorphism on the brain. This model has been shown previously to have motor coordination deficits in the absence of detectable brain iron loading [26], suggesting that HFE deficiency can lead to brain perturbations that are not dependent on iron accumulation within the brain.

In the present study, we report the results from pathway enrichment analyses of transcriptome-wide differences in brain RNA transcript levels in an $Hfe^{-/-}$ mouse model of hemochromatosis relative to wildtype control mice. These analyses identify molecular systems in which high numbers of genes have undergone expression changes.

MATERIALS AND METHODS

Animals

All $Hfe^{+/+}$ and $Hfe^{-/-}$ mice [45] were on an AKR background, which displays a strong iron loading phenotype with regard to liver iron levels and transferrin saturation [46]. Male mice were sacrificed at 9-10 weeks of age following anesthesia (50 mg/kg ketamine, 10 mg/kg xylazine). Organs were collected following transcardial perfusion with isotonic saline. Brains were dissected medially into two hemispheres, immediately snap-frozen in liquid nitrogen, and stored at −80°C. Animal work was conducted at the University of Western Australia and all protocols were approved by the Animal Ethics Committee of the University of Western Australia.

RNA isolation and microarray analysis

Isolation of RNA from brain hemispheres of biological replicates ($n = 8$ mice per group) was performed using TRI reagent (Ambion). Total RNA was purified and concentrated using RNeasy MinElute Kit (Qiagen), quantitated by Quant-iT RiboGreen RNA Quantification Assay (Invitrogen), and amplified and biotin labeled for microarray using the Illumina TotalPrep RNA Amplification Kit (Ambion).

Microarrays were used to assess transcriptome-wide brain transcript levels in biological replicates of $Hfe^{-/-}$ mice and wildtype controls ($n = 4$ per group). Labeled cRNA samples from biological replicates were hybridized to individual arrays on Illumina MouseRef-8 v1.1 Expression BeadChips, which probe over 24,000 transcripts simultaneously. Arrays were scanned using the Illumina BeadArray Reader and BeadScan software.

Data analysis

Performing separate microarrays for each mouse brain sample enabled the wildtype control and $Hfe^{-/-}$ groups to be statistically compared, in order to identify genes with significant mean expression differences. In this paper, the 'expression changes' we refer to are calculated by comparing the mean expression of a gene in $Hfe^{-/-}$ mice to that in wildtype controls. As the choice of normalization and analytical approach can affect the list of genes identified as differentially expressed, four different combinations of normalization and analytical approaches were compared. Microarray data were subjected to either Average or Cubic Spline normalization in BeadStudio v.3 (Illumina) followed by differential expression analysis using either BeadStudio (error model Illumina Custom, differential score |Diff Score|>13, equivalent to $p < 0.05$) or Agilent GeneSpring GX 7.3 (one-way ANOVA, $p < 0.05$). This resulted in differentially-expressed gene lists for each of the four possible combinations of these normalization and analytical approaches, i.e., Cubic Spline/BeadStudio; Average/BeadStudio; Cubic Spline/GeneSpring; Average/GeneSpring. In order to maximize discovery of real expression changes, the results of differential expression analyses were not adjusted for multiple testing [47, 48]. To eliminate probes only detecting non-specific signals, data were filtered to remove probes that returned a mean detection p value >0.01 for both wildtype control and $Hfe^{-/-}$ groups. Detection p value is a BeadStudio measure of the probability of observing a certain level of signal without specific hybridization of the target to the probe.

Pathway classification and enrichment analysis

Single enrichment analyses were performed using the Protein Analysis Through Evolutionary Relationships (PANTHER) Classification System (http://www.pantherdb.org/) and the Database for Annotation, Visualization and Integrated Discovery (DAVID; http://david.abcc.ncifcrf.gov/) [49, 50]. PANTHER classifies genes according to its own curated pathways. DAVID allows the user to choose from a number of publicly available pathway classification databases: we selected the Kyoto Encyclopedia of Genes and Genomes database (KEGG; http://www.genome.jp/kegg/pathway.html) which, in our experience, usually classifies a greater number of genes than the other available options. The inputs for enrichment analyses with PANTHER and DAVID were each of the lists of genes identified as differentially expressed by each of the four different combinations of approaches listed above. A pathway is considered enriched if it is more strongly represented in the list of differentially-expressed genes than would be predicted by chance alone, based on the total

number of genes in the pathway proportionate to the total number of genes on the array. A statistical test (PANTHER uses the binomial statistic, DAVID uses a conservative version of Fisher's Exact test) is used to calculate a p value and pathways with values of $p < 0.05$ are considered to be significantly enriched within the list of differentially-expressed genes.

Additional analyses were performed using Gene Set Enrichment Analysis (GSEA; http://www.broadinstitute.org/gsea/) [51]. The GSEA tool differs from PANTHER and DAVID, which classify a list of genes pre-selected by the user without considering either the direction or the magnitude of expression changes. In contrast, GSEA uses the normalized data values of all probes in the entire microarray dataset. Genes in the dataset are ordered according to the degree of differential expression between the wildtype controls and $Hfe^{-/-}$ mice to create a ranked gene list. The GSEA program then assesses the extent to which members of a particular pathway are concentrated towards either extreme of the ranked gene list; that is, have generally higher expression in control ($Hfe^{+/+}$) mice than $Hfe^{-/-}$ mice or vice versa [51].

We performed GSEA on both Average-normalized and Cubic Spline-normalized array expression datasets. The database used for GSEA was again based on KEGG pathways. To correct for multiple hypothesis testing, the GSEA program randomly permutes either the 'phenotype' labels or 'gene set' (in this case pathway) labels. In accordance with the recommendations in the GSEA user guide for the number of biological replicates in our study, we used 'gene set permutation' rather than 'phenotype permutation' and performed 1000 permutations. The GSEA user guide recommends applying a cut-off of FDR q value <0.25 for generating interesting hypotheses but suggests that a more stringent cut-off may be appropriate when using 'gene set permutation'. We therefore focused on the restricted group of pathways with an FDR q value <0.15 and a nominal p value <0.05.

The 'collapse dataset' option was used for GSEA. When genes are represented on the array by multiple probes, this collapses the probe set into a single data point (the maximum value of the probe set), preventing multiple probes inflating enrichment scores. This can cause errors if the collapsed value does not accurately represent the true value due to inconsistencies between individual probe signals. However the identification of the 'Alzheimer's Disease pathway' and the Notch signaling pathway (see Results) was not due to errors of this kind as most genes in this pathway were detected by single probes or, in the case of multiple probes, showed consistent changes for all probes.

Real-time reverse transcription-polymerase chain reaction

Select transcript changes were further investigated by real-time reverse transcription-polymerase chain reaction (RT-PCR) using additional biological replicates (total $n = 8$ per group). Reverse transcription of RNA to cDNA was performed using the High Capacity cDNA Reverse Transcription Kit (Applied Biosystems). Real-time PCR, using the ABI 7500 Real-Time PCR System (Applied Biosystems), was performed in triplicate reactions using Power SYBR Green PCR Master Mix (Applied Biosystems) and 200 nM sense and antisense primers (supplementary Table 1; available online: http://www.j-alz.com/issues/30/vol30-4.html#supplementarydata02). Levels of transcripts of interest were quantified relative to levels of transcripts for two reference genes, *Actb* and *Rpl13a*. Statistical analysis of real-time RT-PCR results utilized t-testing.

RESULTS

As reported previously [52], $Hfe^{-/-}$ mice showed 3-fold higher liver non-heme iron levels than wildtype $Hfe^{+/+}$ mice, confirming systemic iron loading, but no significant difference in total brain non-heme iron levels, consistent with previous reports of this model on different background strains [26, 27].

Microarray revealed extensive brain gene expression changes in $Hfe^{-/-}$ mice relative to wildtype controls, irrespective of the normalization and analysis approaches used [52]. As a representative example, we present the list of transcripts identified as differentially-expressed by the combination of Average normalization and BeadStudio differential expression analysis (supplementary Data).

Functional classification of gene lists into pathways was initially done using the single enrichment analysis tools PANTHER and DAVID (Materials and Methods). Different combinations of approaches and tools showed some differences in outcomes, reflecting both differences in the gene lists and differences between pathway classification tools, making it difficult to generate a consensus list of enriched pathways. As the example that we consider most representative of the other approaches, we present the full list of pathways significantly enriched within the Average/BeadStudio gene list (supplementary Table 2). It should be noted that in the present context, the term 'pathway', as used

by these bioinformatics pathway classification tools, refers to a collection of molecules in interrelated systems thought to be involved in a particular disease and does not imply a definitive etiological mechanism.

Notably, several pathways were identified irrespective of the approach used, suggesting these are robust findings. These included the general pathway 'Neurodegenerative Diseases' or specific pathways for AD or one or more other neurodegenerative diseases (specifically Parkinson's disease (PD), Huntington's disease (HD) or amyotrophic lateral sclerosis (ALS); supplementary Table 3).

One limitation of tools such as PANTHER and DAVID is that the direction and magnitude of transcript changes are not taken into account. We therefore also analyzed the data using another ontological classification program, GSEA [51], which takes into consideration both the direction and the magnitude of expression changes (see Materials and Methods). In contrast to PANTHER and DAVID, which use restricted subsets of genes chosen by the researcher, GSEA considers the entire normalized microarray dataset.

As detailed in Materials and Methods, supplementary Table 4 shows pathways returning a false discovery rate (FDR) q value below the cut-off recommended for generating interesting hypotheses. However subsequent discussion focuses on pathways passing a more stringent cut-off in both Average- and Cubic Spline-normalized datasets (Table 1).

Both the 'Neurodegenerative Diseases' and 'Alzheimer's Disease' pathways were identified as showing an enrichment of transcript differences in a particular direction in *Hfe*$^{-/-}$ mice (i.e., either mostly higher or mostly lower expression than control mice), irrespective of normalization method (Table 1).

Within each pathway identified, GSEA determines the subset of genes that makes the greatest contribution to the enrichment score, termed the 'core enrichment' group. The full set of 'core enriched' genes in the 'Alzheimer's Disease pathway' for the Average-normalized dataset is shown in Table 2. Similar results were obtained when using the Cubic Spline-normalized dataset (data not shown), with all but one gene in the core enriched group being identified by GSEA for both Average- and Cubic Spline-normalized datasets. (The exception was beta-site-AβPP-cleaving

Table 1
Significantly enriched pathways as determined by gene set enrichment analysis

Pathway	NES	Nominal p value	FDR q value
Notch signaling pathway	1.98	0	0.0118
Type II diabetes mellitus	1.83	0.0014	0.0522
MAPK signaling pathway	1.78	0	0.0605
Wnt signaling pathway	1.73	0	0.0819
Neurodegenerative diseases	1.61	0.0085	0.1424
Alzheimer's disease	1.59	0.0201	0.1422
Long term depression	1.57	0.0103	0.1371

A positive enrichment score indicates a tendency toward higher expression values in the wildtype mice, while a negative enrichment score indicates a tendency toward higher expression values in the *Hfe*$^{-/-}$ mice. Pathways shown here passed a filter of FDR q value <0.15 and nominal p value <0.05 for both Average- and Cubic Spline-normalized datasets. The table displays representative enrichment data from the Average-normalized dataset. NES, normalized enrichment score.

Table 2
Expression changes for genes in the 'Alzheimer's disease pathway'

Gene name and symbol	Fold change	p value
Presenilin 1 *Psen1*	↓5.52	9.6×10^{-6}
Amyloid β (A4) protein precursor *AβPP*	↓1.82	1.2×10^{-5}
Microtubule-associated protein tau *Mapt*	↓2.21	0.0003
Apolipoprotein E *Apoe*	↓1.47	0.0472
Glycogen synthase kinase 3 beta *Gsk3b*	↓2.74	0.0006
Insulin-degrading enzyme *Ide*	↓1.78	0.0226
Caspase 3 *Casp3*	↓5.15	0.0032
Complement component 1, q subcomponent, A chain *C1qa*	↓3.30	0.0006
Complement component 1, q subcomponent, B chain *C1qb*	↓1.63	0.0004
Beta-site AβPP-cleaving enzyme 2 *Bace2*	↓1.34	NS
Anterior pharynx defective 1a homolog *Aph1a*	↓2.66	0.0024
Presenilin enhancer 2 homolog *Psenen*	↓1.37	0.0232
Low density lipoprotein receptor-related protein 1 *Lrp1*	↑1.45	0.0193

Expression changes for genes that were included in the core enriched group of the 'Alzheimer's Disease pathway' (shaded) or those from the pathway that showed significantly altered expression. Genes that are included in the GSEA 'Alzheimer's Disease pathway' but did not show significantly altered expression by microarray were tumor necrosis factor (*Tnf*), interleukin 1 beta (*Il1b*), caspase 7 (*Casp7*), synuclein alpha (*Snca*), alpha-2-macroglobulin (*A2m*), membrane metallo-endopeptidase (*Mme*), amyloid β (A4) protein precursor-binding, family B, member 1 (*Apbb1*), beta-site AβPP-cleaving enzyme 1 (*Bace1*), nicastrin (*Ncstn*), lipoprotein lipase (*Lpl*), and presenilin 2 (*Psen2*). The table displays data generated using the combination of Average normalization and BeadStudio differential expression analysis. Fold change denotes expression in *Hfe*$^{-/-}$ mice relative to wildtype controls. NS, not significant (i.e., $p > 0.05$).

enzyme 2 (*Bace2*), which was identified when Average normalization was used but not Cubic Spline).

The core enriched group may include some genes that do not have significantly altered transcripts yet still contribute to the enrichment score based on fold-change rank and direction. Conversely, the core enriched group does not include genes that have significantly altered transcript levels in the opposite direction to most pathway components. Since such genes may still be relevant (for example, when the genes encoding an inhibitory protein and its target show expression changes in opposite directions), Table 2 also lists all other genes with significantly altered transcript levels in the GSEA 'Alzheimer's Disease pathway'. Of the 24 genes represented on the array which are classified in the 'Alzheimer's Disease pathway', 50% showed significantly altered transcript levels, of which 11 showed significantly decreased levels in $Hfe^{-/-}$ mice relative to wildtype controls for both normalization methods, while only one (low-density lipoprotein receptor-related protein, *Lrp1*) showed significantly increased levels. It is therefore important to recognize that 'enrichment' here reflects a generalized decrease in activity of genes in the 'Alzheimer's disease pathway' in the $Hfe^{-/-}$ mouse brain, as opposed to increased activity. The positions in the KEGG 'Alzheimer's Disease pathway' of proteins encoded by genes showing significantly altered transcript levels are illustrated in Fig. 1.

Relative to wildtype controls, $Hfe^{-/-}$ mice showed decreased brain transcript levels for the genes encoding amyloid-β protein precursor (*AβPP*), presenilin 1

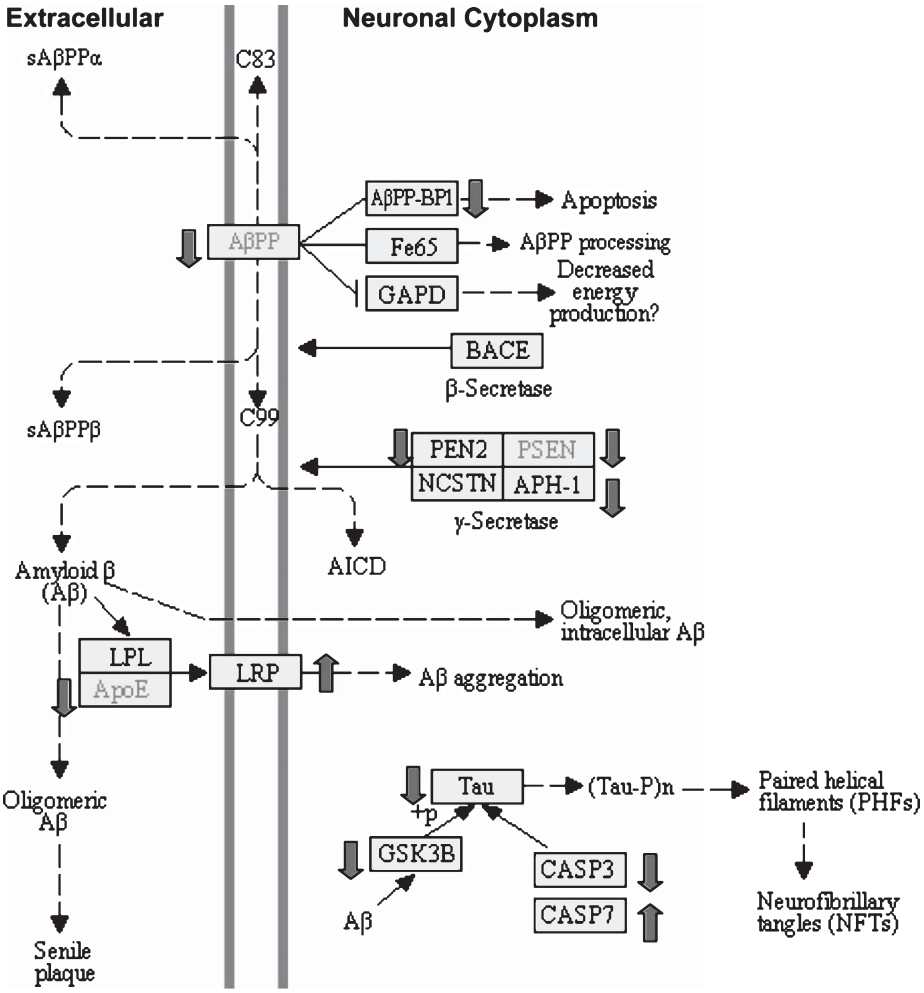

Fig. 1. Altered expression of genes encoding components of the KEGG pathway 'Alzheimer's Disease'. Up arrows indicate genes with significantly higher expression in $Hfe^{-/-}$ brain than wildtype brain ($p < 0.05$), down arrows indicate significantly lower expression. Figure was adapted from KEGG.

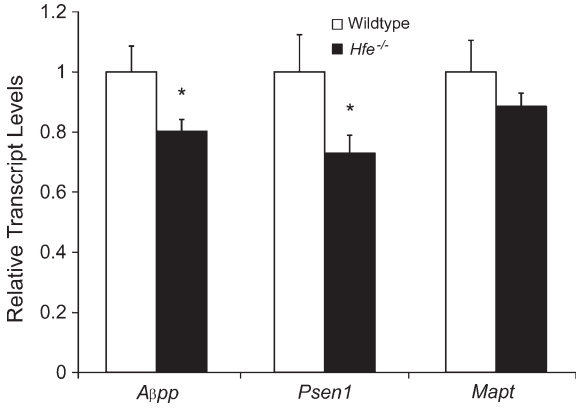

Fig. 2. Real-time RT-PCR validation of expression changes for genes relevant to Alzheimer's disease. Relative levels of transcripts for amyloid-β protein precursor (*AβPP*), presenilin 1 (*Psen1*), and microtubule associated protein tau (*Mapt*) were determined by real-time RT-PCR ($n=8$ per group). Mean expression for wildtype controls was set to 1 and all results standardized accordingly. Error bars represent standard error of the mean. $*p<0.05$.

(*Psen1*), and tau (*Mapt*) (all $p<0.001$, Table 2), all established to be causally associated with AD or other dementias by genetic linkage studies. The $Hfe^{-/-}$ mice also showed decreased brain transcript levels for anterior pharynx defective 1a homolog (*Aph1a*) and presenilin enhancer 2 homolog (*Psenen*), which are essential components of the γ-secretase complex with presenilin 1 [53–55]. Significant down-regulation of *AβPP* and *Psen1* transcript levels in $Hfe^{-/-}$ mice relative to wildtype controls was confirmed in additional biological replicates by real-time RT-PCR (both $p<0.05$, $n=8$ per group, Fig. 2), although the magnitudes of the changes (20–25%) were smaller than those detected by microarray. The changes in *tau* transcript levels detected by microarray were not great enough to reach statistical significance by real-time RT-PCR (Fig. 2).

The genes encoding apolipoprotein E (*Apoe*) and its receptor (*Lrp1*) also showed significantly altered transcript levels by microarray ($p<0.05$), as did other genes relating less directly to AD (Table 2, Fig. 1).

Since the field of AD research is large and very active, pathway updates do not always keep pace with discovery. Table 3 gives changes in transcript levels observed for certain genes not listed in the KEGG 'Alzheimer's Disease pathway' but that are either (i) found to be associated with AD by genome-wide association studies (GWAS) [56, 57] or (ii) listed in the AlzGene database of genes shown through meta-analysis to contain polymorphisms associated with susceptibility to AD [58].

Table 3
Genes with altered expression associated with AD susceptibility

Gene name and symbol	Fold change	*p* value
Cathepsin S *Ctss*	↑1.61	0.0219
Cholinergic receptor, nicotinic, beta polypeptide 2 *Chrnb2*	↑1.36	0.0287
Prion protein *Prnp*	↑1.29	0.0357
Sortilin-related receptor, LDLR class A repeats-containing *Sorl1*	↓1.57	0.0002
Death associated protein kinase 1 *Dapk1*	↓1.59	0.0342
VPS10 domain receptor protein SORCS 1 *Sorcs1*	↓1.79	0.0008
Thyroid hormone receptor alpha *Thra*	↓5.40	9.2×10^{-9}
Transient receptor potential cation channel, subfamily C, member 4 associated protein *Trpc4ap*	↓9.65	2.4×10^{-7}

Expression changes for genes containing single nucleotide polymorphisms that have been associated with susceptibility for Alzheimer's disease. This list was compiled from the AlzGene database and several GWAS. The table displays data generated using the combination of Average normalization and BeadStudio differential expression analysis. Fold change denotes expression in $Hfe^{-/-}$ mice relative to wildtype controls.

Effects on AD genes appear specific in that most of the main known causative genes for other major neurodegenerative diseases (e.g., α-synuclein, parkin 2, superoxide dismutase, huntingtin) did not show robust alterations in transcript levels (data not shown). Identification of other specific neurodegenerative disease pathways (PD, ALS, HD) by DAVID or PANTHER instead usually reflected changes in transcript levels for genes associated with generic neurodegenerative mechanisms, such as actin cytoskeleton or microtubule-related genes or genes involved in mitogen-activated protein kinase (MAPK) signaling. None of these pathways passed the GSEA FDR filter, even with the non-stringent *q* value cut-off of 0.25.

Furthermore, many of the genes driving selection of the 'Neurodegenerative Disease pathway' by GSEA are also relevant to the 'Alzheimer's disease pathway' (e.g., *Psen1*, *AβPP*, *Apoe*, *Mapt*). While the 'Neurodegenerative Disease pathway' contains proteins commonly associated with neural cell death (e.g., various caspases, *Bad*, *Bax*) or reactive astrogliosis (*Gfap*), aside from the cytoskeletal and related transcript changes mentioned above, there was no clear evidence of increased transcripts for these proteins (data not shown). There was also relatively little

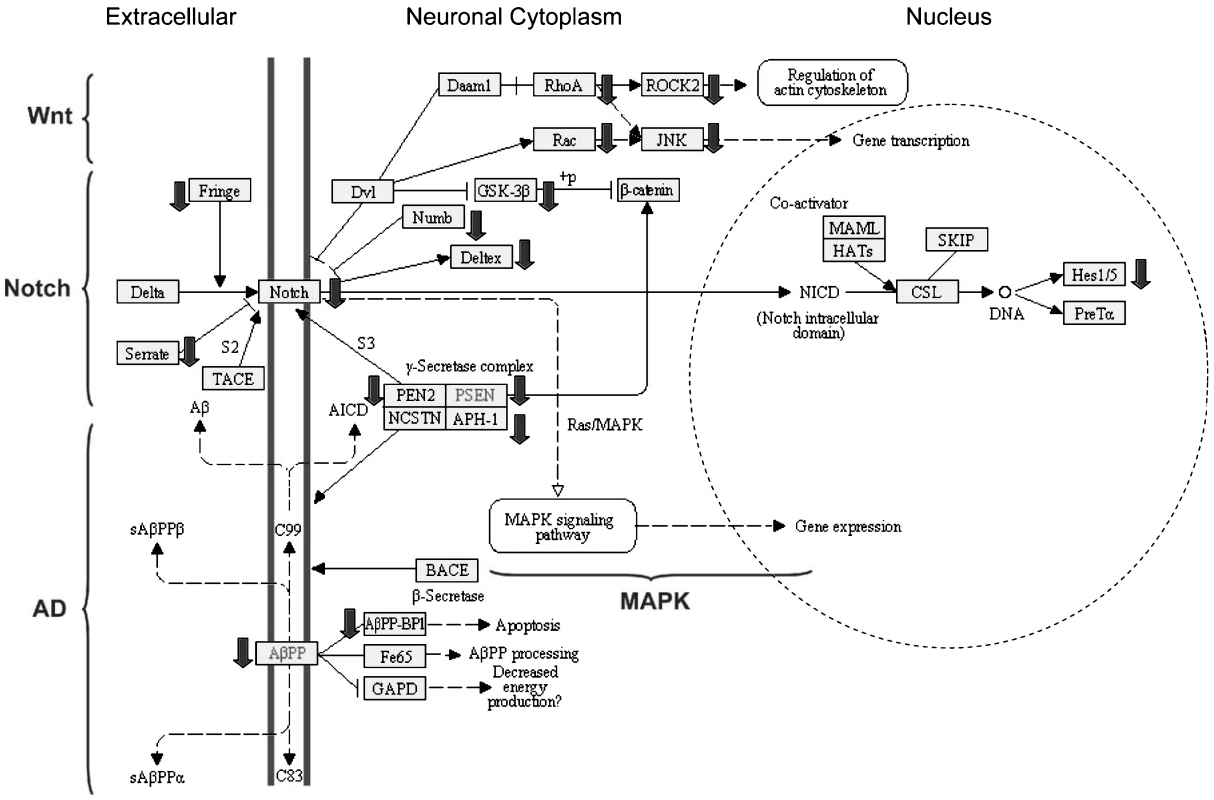

Fig. 3. Interrelationships between different pathways identified as enriched by GSEA. Up arrows indicate genes with significantly higher expression in *Hfe*$^{-/-}$ brain than wildtype brain ($p < 0.05$), down arrows indicate significantly lower expression. The figure was constructed based on KEGG pathways. AD, 'Alzheimer's Disease pathway'.

evidence of changes in transcripts for genes relating to inflammation or oxidative stress.

Several other pathways potentially important in AD were identified by GSEA, including type II diabetes and long-term depression (Table 1). Diabetes is one of the classical symptom triad associated with severe hemochromatosis [59–61] and has also been associated with AD [62, 63]. However the observed expression changes were relatively non-specific in that they affected genes involved in ubiquitous molecular pathways (e.g., genes encoding calcium channels, MAPK signaling molecules) and do not provide clear clues as to potential mechanisms relating to diabetes.

In addition, there were several pathways related to Notch signaling (Table 1, Fig. 3), which contributes to many important CNS phenomena, including developmental neurogenesis, cognition, plasticity, and injury repair [64, 65]. Notch signaling is directly regulated by intramembraneous cleavage of Notch by presenilin. This releases the Notch intracellular domain, which travels to the nucleus and activates target gene transcription. Transcripts for the Notch ligand homolog jagged 2 were lower in *Hfe*$^{-/-}$ brain than wildtype brain (Table 4, Fig. 3) and there was also a reduction in transcripts for the ligand homologs delta-like 1 and 4, although signals for these transcripts were only detected at very low levels (data not shown). There were decreased transcripts for the radical and lunatic fringe homologs (Table 4, Fig. 3), which modulate activation of Notch signal transduction [66].

Importantly, two primary target genes of Notch nuclear signaling by the so-called 'canonical pathway', 'hairy and enhancer of split' 1 and 5 (*Hes1, Hes5*; Fig. 3), showed decreases in transcript levels of between 1.7- and 2-fold by both microarray (Table 4) and real-time RT-PCR (Fig. 4). This provides direct evidence that the observed decreases in transcript levels for the various Notch signaling pathway members and γ-secretase complex components have functional consequences in the form of significant down-regulation of target gene expression.

An important non-canonical function of Notch signaling involves interactions with the wingless/Wnt pathway [67] and regulation of the actin cytoskeleton,

Table 4
Other genes of interest showing significant expression changes

Gene name and symbol	Fold change	*p* value
Notch signaling pathway and related genes		
Jagged 2 *Jag2*	↓4.20	1.04×10^{-5}
Radical fringe gene homolog *Rfng*	↓8.98	4.08×10^{-11}
Lunatic fringe gene homolog *Lfng*	↓2.93	0.0468
Notch gene homolog 3 *Notch3*	↓2.00	0.0042
Hairy and enhancer of split 1 *Hes1*	↓1.72	0.0092
Hairy and enhancer of split 5 *Hes5*	↓2.04	0.0449
Wnt & MAPK signaling and cytoskeletal regulation		
Ras homologue gene family, member A *Rhoa*	↓3.10	0.0006
Rho-associated coiled-coil forming kinase 1 *Rock1*	↓5.60	0.0012
Rho-associated coiled-coil forming kinase 2 *Rock2*	↓17.11	0.0003
RAS-related C3 botulinum substrate 1 *Rac1*	↓2.31	5.95×10^{-9}
RAS-related C3 botulinum substrate 3 *Rac3*	↓3.00	0.0039
Mitogen activated protein kinase 3 *Mapk3*	↓3.12	0.0008
Mitogen activated protein kinase 10 *Mapk10*	↓3.05	8.59×10^{-6}
Mitogen activated protein kinase 14 *Mapk14*	↓1.52	0.0199

The table displays data generated using the combination of Average normalization and BeadStudio differential expression analysis. Fold change denotes expression in $Hfe^{-/-}$ mice relative to wildtype controls.

in particular axon extension [68]. In addition, the Notch signaling pathway cross-talks with the receptor tyrosine kinase/Ras pathway, which feeds into the MAPK signaling pathway [69]. Both the Wnt and MAPK signaling pathways were identified by GSEA (Table 1), while regulation of the actin cytoskeleton was significantly enriched in Average-normalized data (supplementary Table 4).

Furthermore, there are other, more direct connections between cytoskeleton regulation and the Wnt pathway that also tie directly into the MAPK signaling pathway and again genes relating to these pathways showed altered transcript levels in the $Hfe^{-/-}$ brain (Table 4, Fig. 3). Specifically, a sub-pathway

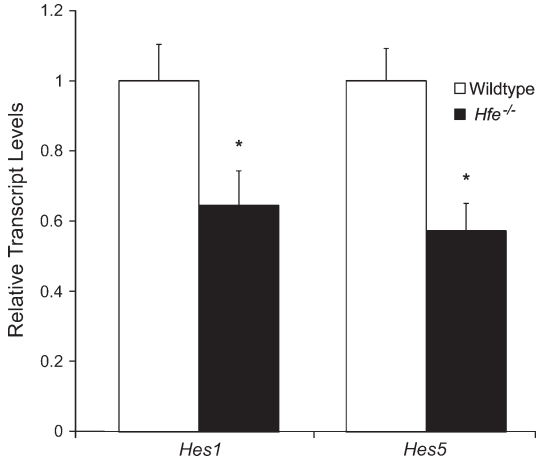

Fig. 4. Real-time RT-PCR validation of expression changes for Notch target genes. Relative levels of *Hes1* and *Hes5* transcripts were determined by real-time RT-PCR ($n = 8$ per group). Mean expression for wildtype controls was set to 1 and all results standardized accordingly. Error bars represent standard error of the mean. $^*p < 0.05$.

of the Wnt signaling pathway generates cytoskeletal changes through ras homolog gene family, member A (*Rhoa*) and Rho-associated coiled-coil forming kinases 1 and 2 (*Rock1, Rock2*) [70]. The *Rocks* and *Rhoa* all showed decreased transcript levels in $Hfe^{-/-}$ brain, as did RAS-related C3 botulinum substrate (*Rac*), another member of this Wnt sub-pathway. Both *Rhoa* and *Rac* activate c-Jun N-terminal kinase (JNK), an important component of the MAPK pathway, and the JNK subcomponent *Mapk10* (JNK3) also showed reduced transcript levels. Other MAPK pathway components showing decreased transcript levels by microarray included subcomponents of both p38 (*Mapk14*) and extracellular signal-regulated kinase ERK 1/2 (*Mapk3*).

DISCUSSION

This study provides the first evidence, by both microarray and real-time RT-PCR, that functional deficiency of the hemochromatosis HFE protein can extensively alter brain transcript levels for genes relating to AD. The findings appear relatively specific for AD-related genes in that few key genes in two other important neurodegenerative diseases, PD and HD, showed altered transcript levels, although there were some changes that may be important in general neurodegenerative processes not specific to any particular disease. The relative lack of effects on genes relating to inflammation suggests most changes in transcripts for AD-related genes observed here are not secondary

to inflammatory changes. A similar lack of effect on genes involved in oxidative stress suggests that the changes are also unlikely to be secondary to oxidative damage.

The observed reductions in brain transcripts for AβPP, presenilin 1, BACE2, and tau in the *Hfe*$^{-/-}$ mouse model of hemochromatosis do not provide clear support for proposals of increased AD risk in human hemochromatosis. Decreases in presenilin 1 and BACE2 would not be expected to exacerbate amyloid-β (Aβ) pathology [71, 72]. Instead decreases in expression of the γ-secretase complex and its substrate AβPP could conceivably retard Aβ production. Decreases in tau transcripts may also protect against AD pathogenesis [73].

If cognitive phenomena attributable to hemochromatosis do occur, these may instead involve mechanisms which are at least partly independent of amyloid or tau pathology or other features of AD pathogenesis. One possibility is that reduced expression of AβPP, tau, presenilin 1, or other AD-related genes may affect important brain functions such as neurogenesis, neuronal function, or brain injury repair throughout life [71, 74–77].

For example, one essential function of presenilin is its role in Notch signal transduction [78–80]. Our findings are consistent with the possibility that decreased expression of presenilin 1 and other γ-secretase complex and Notch signaling pathway components leads to reduced Notch processing and signaling in the *Hfe*$^{-/-}$ brain. The observed decreases in *Hes1* and *Hes5* transcripts (key functional outcomes of Notch canonical signaling), together with changes in transcripts for genes involved in non-canonical pathways regulated through Notch, provide strong evidence for altered Notch signaling. Corresponding changes in humans could have acute consequences at any point in life for memory, learning and other phenomena involving plasticity, as well as potentially compromising injury repair.

It has been proposed that AβPP is the neuronal ferroxidase [81] and might therefore be predicted to increase in response to brain iron loading. Consistent with this, the 5′ untranslated region of AβPP mRNA contains an iron-responsive element [82] which allows regulation of AβPP translation such that translation is increased in response to intracellular iron loading. However, as the *Hfe*$^{-/-}$ brain does not accumulate iron relative to the wildtype AKR mouse brain, this appears unlikely to be relevant in the context of the present study.

While there is no brain iron loading in the *Hfe*$^{-/-}$ mice, there is substantial systemic iron loading. However, overall, the brain transcript changes observed here appear unlikely to reflect acute, indirect effects of systemic iron loading *per se*, since wild-type AKR mice fed a short-term (3 weeks) high iron diet showed no changes in brain transcripts for key AD genes (*AβPP, Psen1, Mapt, Apoe*), despite having systemic iron levels comparable to *Hfe*$^{-/-}$ mice [25]. Possibly there may be other unknown effects of *Hfe* deletion, such as perturbations in copper or other metals, which can also be handled by iron-related proteins.

It is concluded, both on the basis of the mouse data presented here and from previous large studies finding no association between AD and either *HFE* genotype [44] or high serum iron measures [83], that the weight of current evidence does not appear to support substantiative increases in AD risk in patients with *HFE* polymorphisms or high systemic iron levels. The effects reported here might, if anything, be predicted to protect against AD to some extent, since there are no gross changes in brain iron levels in the mouse model used here. However evidence from a recent meta-analysis suggests iron supplementation may be beneficial to attention and concentration across all age groups irrespective of baseline iron levels. More knowledge about the complex relationships involved and the roles of iron and HFE in the brain is therefore required before recommending chelation or other iron-depletion therapies as treatments for neurologic disease, as this will not necessarily improve neurologic functions and may even be harmful in some circumstances.

ACKNOWLEDGMENTS

This work was supported by the University of Newcastle (G0187902) and the National Health and Medical Research Council (NHMRC) of Australia (DT, JKO, RMG). JKO is the recipient of a NHMRC Practitioner Fellowship and DT is the recipient of a NHMRC Senior Research Fellowship.

Authors' disclosures available online (http://www.j-alz.com/disclosures/view.php?id=1212).

REFERENCES

[1] Moos T, Morgan EH (2004) The metabolism of neuronal iron and its pathogenic role in neurological disease: Review. *Ann N Y Acad Sci* **1012**, 14-26.

[2] Zecca L, Youdim MB, Riederer P, Connor JR, Crichton RR (2004) Iron, brain ageing and neurodegenerative disorders. *Nat Rev Neurosci* **5**, 863-873.

[3] Madsen E, Gitlin JD (2007) Copper and iron disorders of the brain. *Annu Rev Neurosci* **30**, 317-337.

[4] Johnstone D, Milward EA (2010) Molecular genetic approaches to understanding the roles and regulation of iron in brain health and disease. *J Neurochem* **113**, 1387-1402.

[5] Burn J, Chinnery PF (2006) Neuroferritinopathy. *Semin Pediatr Neurol* **13**, 176-181.

[6] Gregory A, Polster BJ, Hayflick SJ (2009) Clinical and genetic delineation of neurodegeneration with brain iron accumulation. *J Med Genet* **46**, 73-80.

[7] LeVine SM (1997) Iron deposits in multiple sclerosis and Alzheimer's disease brains. *Brain Res* **760**, 298-303.

[8] Connor JR, Milward EA, Moalem S, Sampietro M, Boyer P, Percy ME, Vergani C, Scott RJ, Chorney M (2001) Is hemochromatosis a risk factor for Alzheimer's disease? *J Alzheimers Dis* **3**, 471-477.

[9] Bartzokis G, Sultzer D, Cummings J, Holt LE, Hance DB, Henderson VW, Mintz J (2000) *In vivo* evaluation of brain iron in Alzheimer disease using magnetic resonance imaging. *Arch Gen Psychiatry* **57**, 47-53.

[10] House MJ, St Pierre TG, Kowdley KV, Montine T, Connor J, Beard J, Berger J, Siddaiah N, Shankland E, Jin LW (2007) Correlation of proton transverse relaxation rates (R2) with iron concentrations in postmortem brain tissue from Alzheimer's disease patients. *Magn Reson Med* **57**, 172-180.

[11] Collingwood JF, Chong RK, Kasama T, Cervera-Gontard L, Dunin-Borkowski RE, Perry G, Posfai M, Siedlak SL, Simpson ET, Smith MA, Dobson J (2008) Three-dimensional tomographic imaging and characterization of iron compounds within Alzheimer's plaque core material. *J Alzheimers Dis* **14**, 235-245.

[12] Ayonrinde OT, Milward EA, Chua AC, Trinder D, Olynyk JK (2008) Clinical perspectives on hereditary hemochromatosis. *Crit Rev Clin Lab Sci* **45**, 451-484.

[13] Feder JN, Gnirke A, Thomas W, Tsuchihashi Z, Ruddy DA, Basava A, Dormishian F, Domingo R Jr, Ellis MC, Fullan A, Hinton LM, Jones NL, Kimmel BE, Kronmal GS, Lauer P, Lee VK, Loeb DB, Mapa FA, McClelland E, Meyer NC, Mintier GA, Moeller N, Moore T, Morikang E, Wolff RK et al. (1996) A novel MHC class I-like gene is mutated in patients with hereditary haemochromatosis. *Nat Genet* **13**, 399-408.

[14] Schmidt PJ, Toran PT, Giannetti AM, Bjorkman PJ, Andrews NC (2008) The transferrin receptor modulates Hfe-dependent regulation of hepcidin expression. *Cell Metab* **7**, 205-214.

[15] West AP Jr, Bennett MJ, Sellers VM, Andrews NC, Enns CA, Bjorkman PJ (2000) Comparison of the interactions of transferrin receptor and transferrin receptor 2 with transferrin and the hereditary hemochromatosis protein HFE. *J Biol Chem* **275**, 38135-38138.

[16] Allen KJ, Gurrin LC, Constantine CC, Osborne NJ, Delatycki MB, Nicoll AJ, McLaren CE, Bahlo M, Nisselle AE, Vulpe CD, Anderson GJ, Southey MC, Giles GG, English DR, Hopper JL, Olynyk JK, Powell LW, Gertig DM (2008) Iron-overload-related disease in HFE hereditary hemochromatosis. *N Engl J Med* **358**, 221-230.

[17] Whitlock EP, Garlitz BA, Harris EL, Beil TL, Smith PR (2006) Screening for hereditary hemochromatosis: A systematic review for the U.S. Preventive Services Task Force. *Ann Intern Med* **145**, 209-223.

[18] Olynyk JK, Hagan SE, Cullen DJ, Beilby J, Whittall DE (2004) Evolution of untreated hereditary hemochromatosis in the Busselton population: A 17-year study. *Mayo Clin Proc* **79**, 309-313.

[19] Adams PC, Passmore L, Chakrabarti S, Reboussin DM, Acton RT, Barton JC, McLaren GD, Eckfeldt JH, Dawkins FW, Gordeuk VR, Harris EL, Leiendecker-Foster C, Gossman E, Sholinsky P (2006) Liver diseases in the hemochromatosis and iron overload screening study. *Clin Gastroenterol Hepatol* **4**, 918-923.

[20] Berg D, Hoggenmuller U, Hofmann E, Fischer R, Kraus M, Scheurlen M, Becker G (2000) The basal ganglia in haemochromatosis. *Neuroradiology* **42**, 9-13.

[21] Nielsen JE, Jensen LN, Krabbe K (1995) Hereditary haemochromatosis: A case of iron accumulation in the basal ganglia associated with a parkinsonian syndrome. *J Neurol Neurosurg Psychiatry* **59**, 318-321.

[22] Bartzokis G, Lu PH, Tishler TA, Peters DG, Kosenko A, Barrall KA, Finn JP, Villablanca P, Laub G, Altshuler LL, Geschwind DH, Mintz J, Neely E, Connor JR (2010) Prevalent iron metabolism gene variants associated with increased brain ferritin iron in healthy older men. *J Alzheimers Dis* **20**, 333-341.

[23] Moos T, Morgan EH (2002) A morphological study of the developmentally regulated transport of iron into the brain. *Dev Neurosci* **24**, 99-105.

[24] Deane R, Zheng W, Zlokovic BV (2004) Brain capillary endothelium and choroid plexus epithelium regulate transport of transferrin-bound and free iron into the rat brain. *J Neurochem* **88**, 813-820.

[25] Johnstone D, Milward EA (2010) Genome-wide microarray analysis of brain gene expression in mice on a short-term high iron diet. *Neurochem Int* **56**, 856-863.

[26] Golub MS, Germann SL, Araiza RS, Reader JR, Griffey SM, Lloyd KC (2005) Movement disorders in the Hfe knockout mouse. *Nutr Neurosci* **8**, 239-244.

[27] Knutson MD, Levy JE, Andrews NC, Wessling-Resnick M (2001) Expression of stimulator of Fe transport is not enhanced in Hfe knockout mice. *J Nutr* **131**, 1459-1464.

[28] Moos T, Trinder D, Morgan EH (2000) Cellular distribution of ferric iron, ferritin, transferrin and divalent metal transporter 1 (DMT1) in substantia nigra and basal ganglia of normal and beta2-microglobulin deficient mouse brain. *Cell Mol Biol (Noisy-le-grand)* **46**, 549-561.

[29] Blacker D, Bertram L, Saunders AJ, Moscarillo TJ, Albert MS, Wiener H, Perry RT, Collins JS, Harrell LE, Go RC, Mahoney A, Beaty T, Fallin MD, Avramopoulos D, Chase GA, Folstein MF, McInnis MG, Bassett SS, Doheny KJ, Pugh EW, Tanzi RE (2003) Results of a high-resolution genome screen of 437 Alzheimer's disease families. *Hum Mol Genet* **12**, 23-32.

[30] Kehoe P, Wavrant-De Vrieze F, Crook R, Wu WS, Holmans P, Fenton I, Spurlock G, Norton N, Williams H, Williams N, Lovestone S, Perez-Tur J, Hutton M, Chartier-Harlin MC, Shears S, Roehl K, Booth J, Van Voorst W, Ramic D, Williams J, Goate A, Hardy J, Owen MJ (1999) A full genome scan for late onset Alzheimer's disease. *Hum Mol Genet* **8**, 237-245.

[31] Collins JS, Perry RT, Watson B Jr, Harrell LE, Acton RT, Blacker D, Albert MS, Tanzi RE, Bassett SS, McInnis MG, Campbell RD, Go RC (2000) Association of a haplotype for tumor necrosis factor in siblings with late-onset Alzheimer disease: The NIMH Alzheimer Disease Genetics Initiative. *Am J Med Genet* **96**, 823-830.

[32] Robson KJ, Lehmann DJ, Wimhurst VL, Livesey KJ, Combrinck M, Merryweather-Clarke AT, Warden DR, Smith AD (2004) Synergy between the C2 allele of transferrin and the

C282Y allele of the haemochromatosis gene (HFE) as risk factors for developing Alzheimer's disease. *J Med Genet* **41**, 261-265.

[33] Lehmann DJ, Schuur M, Warden DR, Hammond N, Belbin O, Kolsch H, Lehmann MG, Wilcock GK, Brown K, Kehoe PG, Morris CM, Barker R, Coto E, Alvarez V, Deloukas P, Mateo I, Gwilliam R, Combarros O, Arias-Vasquez A, Aulchenko YS, Ikram MA, Breteler MM, van Duijn CM, Oulhaj A, Heun R, Cortina-Borja M, Morgan K, Robson K, Smith AD (2012) Transferrin and HFE genes interact in Alzheimer's disease risk: The Epistasis Project. *Neurobiol Aging* **33**, 202; e201-e213.

[34] Kauwe JS, Bertelsen S, Mayo K, Cruchaga C, Abraham R, Hollingworth P, Harold D, Owen MJ, Williams J, Lovestone S, Morris JC, Goate AM (2010) Suggestive synergy between genetic variants in TF and HFE as risk factors for Alzheimer's disease. *Am J Med Genet B Neuropsychiatr Genet* **153B**, 955-959.

[35] Moalem S, Percy ME, Andrews DF, Kruck TP, Wong S, Dalton AJ, Mehta P, Fedor B, Warren AC (2000) Are hereditary hemochromatosis mutations involved in Alzheimer disease? *Am J Med Genet* **93**, 58-66.

[36] Sampietro M, Caputo L, Casatta A, Meregalli M, Pellagatti A, Tagliabue J, Annoni G, Vergani C (2001) The hemochromatosis gene affects the age of onset of sporadic Alzheimer's disease. *Neurobiol Aging* **22**, 563-568.

[37] Candore G, Licastro F, Chiappelli M, Franceschi C, Lio D, Rita Balistreri C, Piazza G, Colonna-Romano G, Grimaldi LM, Caruso C (2003) Association between the HFE mutations and unsuccessful ageing: A study in Alzheimer's disease patients from Northern Italy. *Mech Ageing Dev* **124**, 525-528.

[38] Pulliam JF, Jennings CD, Kryscio RJ, Davis DG, Wilson D, Montine TJ, Schmitt FA, Markesbery WR (2003) Association of HFE mutations with neurodegeneration and oxidative stress in Alzheimer's disease and correlation with APOE. *Am J Med Genet B Neuropsychiatr Genet* **119B**, 48-53.

[39] Berlin D, Chong G, Chertkow H, Bergman H, Phillips NA, Schipper HM (2004) Evaluation of HFE (hemochromatosis) mutations as genetic modifiers in sporadic AD and MCI. *Neurobiol Aging* **25**, 465-474.

[40] Guerreiro RJ, Bras JM, Santana I, Januario C, Santiago B, Morgadinho AS, Ribeiro MH, Hardy J, Singleton A, Oliveira C (2006) Association of HFE common mutations with Parkinson's disease, Alzheimer's disease and mild cognitive impairment in a Portuguese cohort. *BMC Neurol* **6**, 24.

[41] Correia AP, Pinto JP, Dias V, Mascarenhas C, Almeida S, Porto G (2009) CAT53 and HFE alleles in Alzheimer's disease: A putative protective role of the C282Y HFE mutation. *Neurosci Lett* **457**, 129-132.

[42] Percy M, Moalem S, Garcia A, Somerville MJ, Hicks M, Andrews D, Azad A, Schwarz P, Zavareh RB, Birkan R, Choo C, Chow V, Dhaliwal S, Duda V, Kupferschmidt AL, Lam K, Lightman D, Machalek K, Mar W, Nguyen F, Rytwinski PJ, Svara E, Tran M, Wheeler K, Yeung L, Zanibbi K, Zener R, Ziraldo M, Freedman M (2008) Involvement of ApoE E4 and H63D in sporadic Alzheimer's disease in a folate-supplemented Ontario population. *J Alzheimers Dis* **14**, 69-84.

[43] Alizadeh BZ, Njajou OT, Millan MR, Hofman A, Breteler MM, van Duijn CM (2009) HFE variants, APOE and Alzheimer's disease: Findings from the population-based Rotterdam study. *Neurobiol Aging* **30**, 330-332.

[44] Ellervik C, Birgens H, Tybjaerg-Hansen A, Nordestgaard BG (2007) Hemochromatosis genotypes and risk of 31 disease endpoints: Meta-analyses including 66,000 cases and 226,000 controls. *Hepatology* **46**, 1071-1080.

[45] Zhou XY, Tomatsu S, Fleming RE, Parkkila S, Waheed A, Jiang J, Fei Y, Brunt EM, Ruddy DA, Prass CE, Schatzman RC, O'Neill R, Britton RS, Bacon BR, Sly WS (1998) HFE gene knockout produces mouse model of hereditary hemochromatosis. *Proc Natl Acad Sci U S A* **95**, 2492-2497.

[46] Fleming RE, Holden CC, Tomatsu S, Waheed A, Brunt EM, Britton RS, Bacon BR, Roopenian DC, Sly WS (2001) Mouse strain differences determine severity of iron accumulation in Hfe knockout model of hereditary hemochromatosis. *Proc Natl Acad Sci U S A* **98**, 2707-2711.

[47] Bender R, Lange S (2001) Adjusting for multiple testing–when and how? *J Clin Epidemiol* **54**, 343-349.

[48] Rothman KJ (1990) No adjustments are needed for multiple comparisons. *Epidemiology* **1**, 43-46.

[49] Huang da W, Sherman BT, Lempicki RA (2009) Systematic and integrative analysis of large gene lists using DAVID bioinformatics resources. *Nat Protoc* **4**, 44-57.

[50] Dennis G Jr, Sherman BT, Hosack DA, Yang J, Gao W, Lane HC, Lempicki RA (2003) DAVID: Database for Annotation, Visualization, and Integrated Discovery. *Genome Biol* **4**, P3.

[51] Subramanian A, Tamayo P, Mootha VK, Mukherjee S, Ebert BL, Gillette MA, Paulovich A, Pomeroy SL, Golub TR, Lander ES, Mesirov JP (2005) Gene set enrichment analysis: A knowledge-based approach for interpreting genome-wide expression profiles. *Proc Natl Acad Sci U S A* **102**, 15545-15550.

[52] Johnstone D, Graham RM, Trinder D, Delima RD, Riveros C, Olynyk JK, Scott RJ, Moscato P, Milward EA (2012) Brain transcriptomic perturbations in the $Hfe^{-/-}$ mouse model of genetic iron loading. *Brain Res*, **1448**, 144-152.

[53] Pardossi-Piquard R, Yang SP, Kanemoto S, Gu Y, Chen F, Bohm C, Sevalle J, Li T, Wong PC, Checler F, Schmitt-Ulms G, St George-Hyslop P, Fraser PE (2009) APH1 polar transmembrane residues regulate the assembly and activity of presenilin complexes. *J Biol Chem* **284**, 16298-16307.

[54] Shirotani K, Edbauer D, Prokop S, Haass C, Steiner H (2004) Identification of distinct gamma-secretase complexes with different APH-1 variants. *J Biol Chem* **279**, 41340-41345.

[55] Francis R, McGrath G, Zhang J, Ruddy DA, Sym M, Apfeld J, Nicoll M, Maxwell M, Hai B, Ellis MC, Parks AL, Xu W, Li J, Gurney M, Myers RL, Himes CS, Hiebsch R, Ruble C, Nye JS, Curtis D (2002) aph-1 and pen-2 are required for Notch pathway signaling, gamma-secretase cleavage of betaAPP, and presenilin protein accumulation. *Dev Cell* **3**, 85-97.

[56] Grupe A, Abraham R, Li Y, Rowland C, Hollingworth P, Morgan A, Jehu L, Segurado R, Stone D, Schadt E, Karnoub M, Nowotny P, Tacey K, Catanese J, Sninsky J, Brayne C, Rubinsztein D, Gill M, Lawlor B, Lovestone S, Holmans P, O'Donovan M, Morris JC, Thal L, Goate A, Owen MJ, Williams J (2007) Evidence for novel susceptibility genes for late-onset Alzheimer's disease from a genome-wide association study of putative functional variants. *Hum Mol Genet* **16**, 865-873.

[57] Poduslo SE, Huang R, Huang J, Smith S (2009) Genome screen of late-onset Alzheimer's extended pedigrees identifies TRPC4AP by haplotype analysis. *Am J Med Genet B Neuropsychiatr Genet* **150B**, 50-55.

[58] Bertram L, McQueen MB, Mullin K, Blacker D, Tanzi RE (2007) Systematic meta-analyses of Alzheimer disease genetic association studies: The AlzGene database. *Nat Genet* **39**, 17-23.

[59] Beutler E (2006) Hemochromatosis: Genetics and pathophysiology. *Annu Rev Med* **57**, 331-347.
[60] Pietrangelo A (2004) Hereditary hemochromatosis - a new look at an old disease. *New Engl J Med* **350**, 2383-2397.
[61] O'Neil J, Powell L (2005) Clinical aspects of hemochromatosis. *Semin Liver Dis* **25**, 381-391.
[62] Luchsinger JA, Gustafson DR (2009) Adiposity, type 2 diabetes, and Alzheimer's disease. *J Alzheimers Dis* **16**, 693-704.
[63] Bruce DG, Davis WA, Casey GP, Starkstein SE, Clarnette RM, Foster JK, Almeida OP, Davis TM (2008) Predictors of cognitive impairment and dementia in older people with diabetes. *Diabetologia* **51**, 241-248.
[64] Lathia JD, Mattson MP, Cheng A (2008) Notch: From neural development to neurological disorders. *J Neurochem* **107**, 1471-1481.
[65] Selkoe D, Kopan R (2003) Notch and Presenilin: Regulated intramembrane proteolysis links development and degeneration. *Annu Rev Neurosci* **26**, 565-597.
[66] Yang LT, Nichols JT, Yao C, Manilay JO, Robey EA, Weinmaster G (2005) Fringe glycosyltransferases differentially modulate Notch1 proteolysis induced by Delta1 and Jagged1. *Mol Biol Cell* **16**, 927-942.
[67] Fischer A, Gessler M (2007) Delta-Notch–and then? Protein interactions and proposed modes of repression by Hes and Hey bHLH factors. *Nucleic Acids Res* **35**, 4583-4596.
[68] Giniger E (1998) A role for Abl in Notch signaling. *Neuron* **20**, 667-681.
[69] Hurlbut GD, Kankel MW, Artavanis-Tsakonas S (2009) Nodal points and complexity of Notch-Ras signal integration. *Proc Natl Acad Sci U S A* **106**, 2218-2223.
[70] Maekawa M, Ishizaki T, Boku S, Watanabe N, Fujita A, Iwamatsu A, Obinata T, Ohashi K, Mizuno K, Narumiya S (1999) Signaling from Rho to the actin cytoskeleton through protein kinases ROCK and LIM-kinase. *Science* **285**, 895-898.
[71] De Strooper B (2007) Loss-of-function presenilin mutations in Alzheimer disease. Talking Point on the role of presenilin mutations in Alzheimer disease. *EMBO Rep* **8**, 141-146.
[72] Dominguez D, Tournoy J, Hartmann D, Huth T, Cryns K, Deforce S, Serneels L, Camacho IE, Marjaux E, Craessaerts K, Roebroek AJ, Schwake M, D'Hooge R, Bach P, Kalinke U, Moechars D, Alzheimer C, Reiss K, Saftig P, De Strooper B (2005) Phenotypic and biochemical analyses of BACE1- and BACE2-deficient mice. *J Biol Chem* **280**, 30797-30806.
[73] Roberson ED, Scearce-Levie K, Palop JJ, Yan F, Cheng IH, Wu T, Gerstein H, Yu GQ, Mucke L (2007) Reducing endogenous tau ameliorates amyloid beta-induced deficits in an Alzheimer's disease mouse model. *Science* **316**, 750-754.
[74] Milward EA, Papadopoulos R, Fuller SJ, Moir RD, Small D, Beyreuther K, Masters CL (1992) The amyloid protein precursor of Alzheimer's disease is a mediator of the effects of nerve growth factor on neurite outgrowth. *Neuron* **9**, 129-137.
[75] Small DH, Clarris HL, Williamson TG, Reed G, Key B, Mok SS, Beyreuther K, Masters CL, Nurcombe V (1999) Neurite-outgrowth regulating functions of the amyloid protein precursor of Alzheimer's disease. *J Alzheimers Dis* **1**, 275-285.
[76] Harada A, Oguchi K, Okabe S, Kuno J, Terada S, Ohshima T, Sato-Yoshitake R, Takei Y, Noda T, Hirokawa N (1994) Altered microtubule organization in small-calibre axons of mice lacking tau protein. *Nature* **369**, 488-491.
[77] Saura CA, Choi SY, Beglopoulos V, Malkani S, Zhang D, Shankaranarayana Rao BS, Chattarji S, Kelleher RJ 3rd, Kandel ER, Duff K, Kirkwood A, Shen J (2004) Loss of presenilin function causes impairments of memory and synaptic plasticity followed by age-dependent neurodegeneration. *Neuron* **42**, 23-36.
[78] Struhl G, Greenwald I (2001) Presenilin-mediated transmembrane cleavage is required for Notch signal transduction in Drosophila. *Proc Natl Acad Sci U S A* **98**, 229-234.
[79] Brunkan AL, Goate AM (2005) Presenilin function and gamma-secretase activity. *J Neurochem* **93**, 769-792.
[80] De Strooper B (2003) Aph-1, Pen-2, and Nicastrin with Presenilin generate an active gamma-Secretase complex. *Neuron* **38**, 9-12.
[81] Duce JA, Tsatsanis A, Cater MA, James SA, Robb E, Wikhe K, Leong SL, Perez K, Johanssen T, Greenough MA, Cho HH, Galatis D, Moir RD, Masters CL, McLean C, Tanzi RE, Cappai R, Barnham KJ, Ciccotosto GD, Rogers JT, Bush AI (2010) Iron-export ferroxidase activity of beta-amyloid precursor protein is inhibited by zinc in Alzheimer's disease. *Cell* **142**, 857-867.
[82] Rogers JT, Randall JD, Cahill CM, Eder PS, Huang X, Gunshin H, Leiter L, McPhee J, Sarang SS, Utsuki T, Greig NH, Lahiri DK, Tanzi RE, Bush AI, Giordano T, Gullans SR (2002) An iron-responsive element type II in the 5′-untranslated region of the Alzheimer's amyloid precursor protein transcript. *J Biol Chem* **277**, 45518-45528.
[83] Milward EA, Bruce DG, Knuiman MW, Divitini ML, Cole M, Inderjeeth CA, Clarnette RM, Maier G, Jablensky A, Olynyk JK (2010) A cross-sectional community study of serum iron measures and cognitive status in older adults. *J Alzheimers Dis* **20**, 617-623.